Polymer Bulletin (2024) 81:12819–12840
https://doi.org/10.1007/s00289-024-05317-7

ORIGINAL PAPER

Biocomposites based on polypropylene and Agave fibers (*Agave Americana L*): investigation on physical, thermal and mechanical properties

Afef Mansouri[1] · Jalel Ben Nasr[2] · Mohamed Ben Amar[1]

Received: 31 March 2023 / Revised: 11 May 2024 / Accepted: 13 May 2024 /
Published online: 25 May 2024

Abstract

This study is a comparative assessment of polypropylene composites reinforced with two different range size of Agave Americana fibers. The first is from 125 to 630 microns, named as Short Agave Fiber (SHAF), and the second range is beyond 630 microns, named as Long Agave Fiber (LAF). The composites were produced by twin-screw extrusion and injection molding processes. The composite manufacturing by this interior part of plant agave fibers is mentioned in the first time in the literature. The fiber content for the SHAF and LAF composites was chosen as 10 wt. %. It was found that better mechanical properties were achieved with LAF composite which increased by 301.4% compared with the neat PP. This was explained by LAF features compared to SHAF such as the higher cellulose content LAF (73.5%) and SHAF (40.3%), the higher crystallinity index was obtained better thermal stability which led to a composite which is more crystalline, more thermally stable and stiffer. This was explained by the good interfacial adhesion between fibers and the matrix revealed by SEM analysis.

✉ Afef Mansouri
afeffmansouri@gmail.com

[1] Electromechanical Systems Laboratory, LASEM, National Engineering School of Sfax, University of Sfax, Soukra Km 4, 3038 Sfax, Tunisia

[2] Research Unit Advanced Materials, Applied Mechanics, Innovative Processes and Environment, (UR22ES04), Higher Institute of Applied Sciences and Technology of Gabes, University of Gabes, 6072 Gabes, Tunisia

Graphical abstract

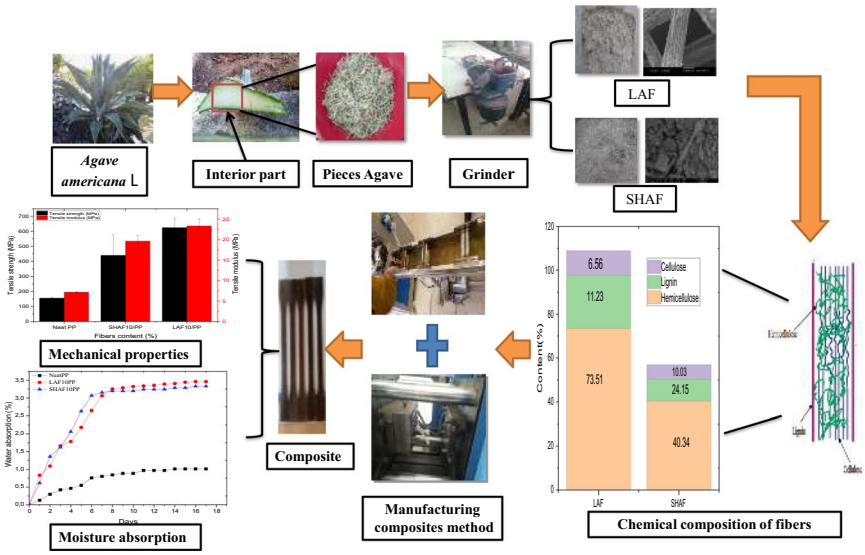

Keywords Polypropylene · Agave fibers · Composites · Extrusion · Injection molding · Mechanical properties · Characterizations

Introduction

Due to the increasing pollution caused by the use of plastics materials, several attentions in the field of materials have turned to the generation of biodegradable material sources.

Biocomposites play an important role in developing biodegradable materials that meet both design requirements and customer goals. They have become available alternatives to synthetic plastic materials because they are usually recyclable and generally exhibit a higher degree of biodegradability with lower impacts on climate change and lower toxicities [1–4]. The most common biocomposites are manufactured with several types of matrices such as petrochemical origin (High density polyethylene [5], poly(ethylene oxide) [6], poly(vinyl chloride) [7], poly(methyl methacrylate) [4, 5], poly(styrene) [8], poly(urethane) [9], poly(propylene) [10] and biopolymer (PLA) [6, 7], and polyhydroxyalkanoates(PHAs) [11, 12] reinforced with natural fibers. Among these types of plastics, the polypropylene (PP) is widely used in various fields such as packaging, building materials and the automotive industry because of its excellent heat resistance, thermal stability, non-toxicity and low cost [13–17]. The properties of PP were modified using reinforcement natural fiber in order to optimize their physical properties and improve their mechanical performance [16, 18–21]. Many advantages of natural fibers called the attention

of many researchers to the use of plant-derived fibers as reinforcing agent in polymeric materials. It has been reported that natural fibers composites exhibit higher mechanical performances including high strength and stiffness [22] compared to neat thermoplastic matrix. In fact, lignocellulosic fibers are available in large quantities around the world and offer many advantages such as biodegradability, recyclability, lower cost, low density, non-toxicity and reduced impact on the environment [23]. Additional benefits include energy savings, resource renewal capacity, and good thermal and mechanical properties [24]. The main components of fibers are cellulose, hemicelluloses and lignin. They contain a major rate of cellulose, which enhances the mechanical properties of fibers [25]. The main types of lignocellulosic fibers are classified according to their location in the plant, for example: bast fibers (jute [26], kenaf [27], ramie [28], hemp [29], and flax [30]), leaf fibers (agave, abaca, sisal, and pineapples [31]), seed fibers (cotton, coir, and kapok [32]), fruit fibers (fiber coconut [33]), grass and reed fiber (wheat, rice, and maize [31]), and other types (wood [22]).

The lignocellulosic fibers used in this work are the fibers extracted from the leaf of plant *Agave Americana L.* Common names of *Agave americana* are *American aloe* or *maguey*. Common names of Agave americana are American aloe or maguey. Agave belongs to the monocotyledonous family called Agaveceae [34]. *Agave americana* flourishes in South Africa as well as the Mediterranean area [35], in Tunisia. This plant is the most abundant variety of agave. Before the manufacturing of the composites reinforced with agave fiber, it is necessary to apply a suitable method of fiber extraction. The Agave fibers can be extracted by several methods such as retting in water [36], retting in seawater [37], retting in soil [38], chemical extraction [39], biological extraction (use of bacteria and enzymes) [40] and decortication method [41, 42]. The retting in seawater or water consists in putting the Agave leaves in seawater or water [43, 44]. Sea water and water retting methods are not environmentally sound at an industrial scale due to the large volume of polluted water corruption and squandering of water. Also, the unpleasant smell produced by the anaerobic fermentation [30], as well as the high costs of labor and drying caused by water retting [45]. Retting in soil method rests on the activity of microorganisms in the soil [38]. Enzymatic retting has not yet reached industry scale due to high costs [46]. Chemical method had been also using by Jaouadi et al., which consists on immersing the Agave leaves with a hydrolysis treatment [39]. This process leads to the degradation of the cell wall, which is detrimental to the mechanical properties of the isolated fibers. In fact, the properties of composite reinforced with natural fibers depend of many factor such as extraction method, fiber content, fiber dispersion, fiber orientation, and matrix selection [47]

Most of the work on agave composites investigated the influence of added agave fiber on mechanical properties. In this context, Torres-tello et al. [48] have elaborated composites based on poly(hydroxybutyrate) (PHB) and poly(hydroxybutyrate-co-hydroxy-valerate) P (HB-HV) reinforced Agave bagasse fiber waste product of industry with size between 297 and 400 µm. They proved that tensile and flexural strength were not negatively affected by fiber addition. The same type of fiber and with the same size was also used by Cisneros-Lopez [49] to study the effect of fiber surface treatment on the mechanical properties of rotomolded poly(ethylene)-agave

fiber composites. This author made a comparative study of poly(lactic acid)/agave fiber biocomposites produced by rotational molding and compression molding in a recent research [50].

In this work, the Agave Americana L was extracted by mechanical method and the interior part of the plant was ground and sieved. Two sizes of Agave fiber were used: The first one is between 125 and 630 µ (SHAF), and the second is beyond 630 µ (LAF). However, the extraction method, interior part of the Agave plant and the sizes of Agave fiber were not yet mentioned in the literature for the production of PP composites. This study aims to compare the effectiveness of Long Agave Fiber (LAF) and Short Agave Fiber (SHAF) as reinforcing agent in PP composites produced by twin-screw extrusion and injection molding processes.

Materials and methods

The Agave leaves (Fig. 1a) used in this study were collected from Sousse (Tunisia), washed into water to remove any remaining unwanted materials. The interior part of agave's leaf is cut into pieces (see Fig. 1b). They were subsequently dried in the oven at 70 °C up to constant weight. Then, they were grinded and sieved (Fig. 1c). Two sizes of Agave fiber were used: The first one is between 125 and 630 microns (Fig. 1d), and the second is beyond 630 microns (Fig. 1e). Then, fibers were stocked in black plastic bags to protect them from moisture and light.

The matrix used is PP (CERTENE PMB35). It is a PP-based thermoplastic polymer designed for injection molding and was bought from Techno polymer society,

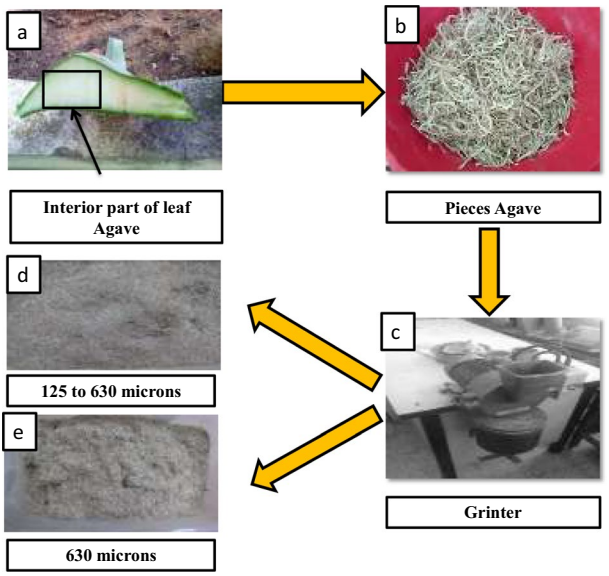

Fig. 1 Mechanical extraction fibers of *Agave Americana L.*

Sfax-Tunisia. The density provided in the technical data sheet of this polymer was 0.9, and its melt flow rate was 35 g/10 min.

Chemical properties of fibers

The determination of the basic chemical composition was determined following ASTM standard protocols. Samples were first submitted to reflux extraction with ethanol/toluene (ASTM D 1107-56) to determine the extractable rate. The amount of lignin, holocellulose, cellulose and ash were determined according to ASTM D 1106-56, ASTM D 1104-56, ASTM D 1103-60 and ASTM D 1102-84 standards, respectively.

A Fourier Transform-infrared spectroscopy (ATR-FTIR) of fibers was carried out using a PerkinElmer instrument at room temperature. The wave number range is from 4000 cm^{-1} to 400 cm^{-1} recorded with 16 scans with a resolution of 4 cm^{-1}.

The samples of fibers were subjected to the X-ray diffraction (XRD) analysis using an Xpert-Pro diffractometer with diffracted intensity of Cu Kα radiation with a wave length of 0.154 nm. The range of 2θ is between 10° and 60°.

The XRD was used to determine the crystallinity index (I_{Cr})) has been computed via Segal method given by Eq. (1) at the height of the (200) peak ((I_{200}) $2\theta = 22.7°$) and the minimum between the (200) and (110) peaks ((I_{AM}) $2\theta = 18°$). I_{200} represents both crystalline and amorphous materials, while I_{AM} represents only amorphous materials [51].

$$I_{cr} = \left[\frac{(I_{200} - I_{AM})}{I_{200}}\right] \times 100 \tag{1}$$

Crystallite size (D) was determined by following Scherer's [52] equation:

$$D = \frac{K\lambda}{\beta \cos\theta} \tag{2}$$

where L is the crystallite size perpendicular to the plane; $K = 0.89$, is the Sharer's constant, $\lambda = 0.1541$ nm is the wavelength of the radiation, β is the peak's full-width half-maximum (FWHM) in radians, and θ is the Bragg angle.

The crystallographic spacing (d) was calculated by following Bragg's [53] equation

$$\lambda = 2d \sin\theta \tag{3}$$

Physical properties of fibers

The thermal analysis was performed on about 2 mg of fiber samples and on 5–7 mg of composite samples using a PerkinElmer (Pyris 6 TGA) analyzer by under nitrogen atmosphere. The samples were heated from 30 °C to 700 °C at a heating rate of 10 °C/min.

Observation of the microstructure of fibers was as well as the fractured sections of film samples used during tensile testing were performed by scanning electron microscope (Jeol, JSM-540).

Composite preparation

Agave fibers-polypropylene composites with 10 wt% of LAF and SHAF content were melt compounded using twin-screw extruder. The temperature profile of the extruder barrel was set to 170, 180, 180, 180, 190, and 200 °C. The screw speed was set at 100 rpm, and the feeding rate was 2 kg/h. For each condition, 10 wt% fibers were added to the matrix. The extrudates were then cooled in a bath water and cut into pellets with a plastic crusher. The pellets latter were placed on the oven set at 60 °C for 24 h prior to injection molding. Specimens according to ISO-527-2 standard were produced.

Mechanical properties of composite

Tensile tests of composite were performed with a WDW-5 Universal Electromechanical Testing Machine. The load cell was 5 kN. The crosshead speed was set at 2mm/min. Displacement was measured using an extensometer. Samples have a gauge length about of 50 mm and a thickness about 4 mm. The measurement was repeated at least 5 times for samples, and the average of three sample readings was taken for accurate results.

Physical properties of composite

Differential scanning calorimetry (DSC) analysis of composite was performed on 3–5mg samples of composite pellets using a PerkinElmer DSC 4000. The composite samples were first heated from 30 to 400°C with a heating rate of 20°C/min under nitrogen flux about 20ml/min. The samples were then cooled from 400 to 20 °C at a cooling rate of 20 °C/min.

The crystallinity index was calculated using the following Eq. (2):

$$X_C(\%) = \left(\frac{\Delta H_f}{\Delta H_{f_0}}\right) \times 100 \tag{4}$$

where $\Delta H_{f0} = 209$ J/g for 100% crystalline PP [54] and ΔH_f is the fusion enthalpy of the sample.

Specimens were first dried in the oven at 50 °C for 24 h and then cooled in a desiccator. After that, they were immerged in distilled water. The weights of the samples were measured every day up to 18 days. The water absorption of the composites was conducted by applying the following equation:

$$\text{Water absorption}(\%) = \left[\frac{(W_t - W_0)}{W_0}\right] \times 100 \quad (5)$$

where W_0 is the initial weight of the sample, and W_t is the weight in time t.

The density of composite pellets was calculated using a pycnometer and the ethanol as the liquid of immersion. Examined samples were dried in the oven at 50 °C for 24 h to remove moisture.

The density was computed using Eq. (4):

$$\rho_f = \frac{(m_3 - m_1)}{[(m_2 - m_1) - (m_4 - m_3)]}\rho_e \quad (6)$$

where

ρ_e is the density of ethanol at 25 °C.
m_1 is the weight of the empty pycnometer.
m_2 is the weight of the pycnometer filled with ethanol at 25°C.
m_3 is the weight of the pycnometer filled with chopped samples.
m_4 is the weight of the pycnometer filled with chopped sample and ethanol.

Results and discussion

Chemical properties

Fibers Agave is composed of three main compounds: cellulose, hemicelluloses, and lignin. The cellulose in LAF and SHAF was 73.5 and 40.3%, respectively. The LAF obtained by mechanical extraction showed a higher value of cellulose content compared to another type of Agave such as Agave fourcroydes (72% cellulose)[55]. In addition, the cellulose of LAF is higher compared to the after burial in soil and distilled water extraction methods. The former methods yielded 63.12 and 68.54% of cellulose content, respectively [38, 56]. Thus, the mechanical extraction was found the most efficient method. LAF has higher cellulose content compared to SHAF. Better tensile strength and Young's modulus could be reached for LAF [57]. The hemicelluloses were 11.2 and 24.2% for the LAF and SHAF, respectively. In a previous work of Oudiani et al. [58], the hemicelluloses content obtained from *Agave Americana L* treated with NaOH concentrations at 1% and 10% was almost 27% for both concentrations. The low content of hemicelluloses in this present work represents another advantage to the fiber's quality. Indeed, the least hemicelluloses content was, the stronger the fiber becomes. In fact, its presence with high quantities leads to the degradation and the disintegration of micro-fibers [59]. The lignin content of LAF and SHAF was 6.6 and 10.0%. Lignin presents many advantages, e.g., can act as a shield against biological attack [60]. In addition, it plays an important role in protecting the hemicellulose and cellulose. However, it is well known for its negative impact on fiber structure, property and morphology[61]. The ash content of

LAF (1.6%) and SHAF (4.5%) was lower than that founded by Yang and Pan yielded 5.3% [62].

FTIR analysis

Figure 2 presents the FTIR analysis of LAF and SHAF, a broad absorption band in the area 3600–3000 cm^{-1} due to the presence of O–H. According to Sathishkumar et al. [63], these can be attributed to the cellulose $I_{\beta,}$ which is due to the presence of cellulose *I* structure in LAF and SHAF. These findings were confirmed by the X-ray analysis below. However, the two bands at 2921 and 2846 cm^{-1}, assigned to CH and CH_2, would be attributed to the cellulose and hemicelluloses [63–65]. The small sharper peaks at 2096 to 2323 cm^{-1} would correspond to the asymmetrical vibrations confirming the presence of waxes. A similar peak was reported for the *Calotropis gigantea* fibers at 2133 cm^{-1} [66]. According to Taktak et al. [22], the small protrusion at 1735 cm^{-1}can be attributed to the presence of lignin, and/or ester group in hemicelluloses. The intense peak at 1600 cm^{-1} can be associated with the presence of lignin [67] and/or due to the presence of water in the fibers. According to Pereira et al., the bands at 1411, 1370 and at 1317 cm^{-1} could be interpreted as indicators of crystalline cellulose, but the peak at 923 cm^{-1}could be due to the amorphous cellulose [38]. These characteristic peaks prove the crystallinity of LAF and SHAF. This will be further confirmed by the analysis of the XRD. With total agreement with Reddy et al. [68], the small peak localized at 1248 cm^{-1}would correspond to the –COO can be attributed to presence of hemicellulose. Also, the intense peak at 1017 cm^{-1} can be attributed to the C–O and OH could be due to the presence in cellulose [69]. According to De Rose et al. [69], the small peak at 923 cm^{-1} may be due to the presence of cellulose showing C–O–C stretching vibration

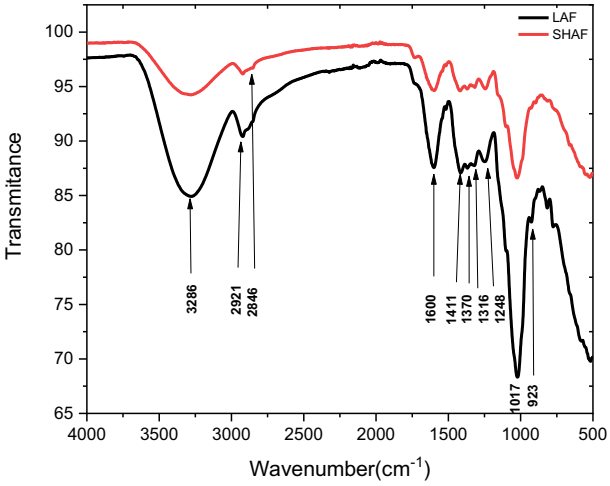

Fig. 2 FTIR spectrum of LAF and SHAF

Table 1 Characteristic FTIR peak positions of LAF and SHAF fibers

Samples	Wave number (cm^{-1})	Vibrational mode(s)
LAF	3002–3657	O–H stretching
	2921	C–H stretching
	2846	C–H2 stretching
	1248	–COO stretching
	1017	C–O and OH stretching
	923	C–O–C stretching
SHAF	3010–3632	O–H stretching
	2930	C–H stretching
	2846	C–H2 stretching
	1236	–COO stretching
	1006	C–O and OH stretching

of β, 1,4 glycosidic linkages triggered by cellulose. The distinguishable peak values corresponding to the functional group interaction are presented in Table 1.

XRD analysis

Figure 3 shows the XRD spectrum of LAF and SHAF. The presence of the 4 localized peaks 2θ such as 15°, 16.7°, and 22.2° represents, respectively, the diffraction angle of the Miller indices' plane (1–10), (110), and (200) characteristic of the native cellulose I [70].

The intense peak at 2θ equal to 22.2° can be attributed to crystallographic plane (200) which indicates the crystalline part (cellulose). The small peak at 34.8° can be

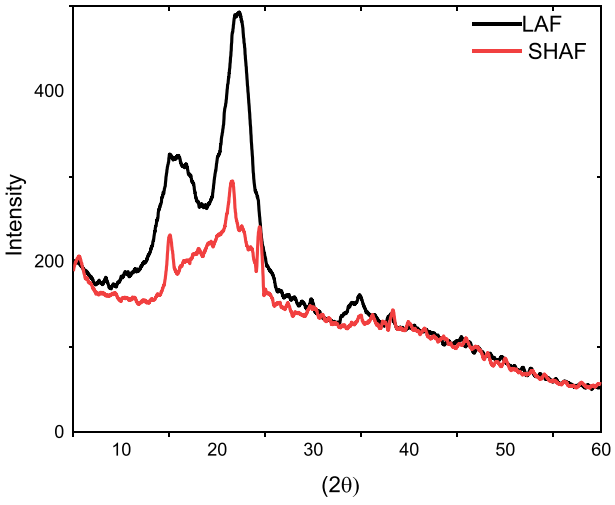

Fig. 3 X-ray spectrum of LAF and SHAF

assigned to a quarter of the length of one cellobiose unit also arises from ordering along the fiber direction [71].

The crystallinity index, lattice spacing (d) and crystal size (D) of LAF and LAF have been calculated by using Eqs. (1)–(3), respectively, and the corresponding values are presented in Table 2. The next result was related to the crystallinity index of the LAF and SHAF which was 51.0 and 30.4%, respectively. This crystallinity index of LAF differs with other extraction methods. It was found 41.0 and 50.0% for *Agave Americana* after retting in seawater and in distilled water, respectively [58]. Also, the crystallinity index of LAF (51%) is height compared with *Lygeum spartum* fibers (46.2%) and *Ferula communis* fibers (48%) [72]. Other studies revealed less crystallinity indices compared SHAF fibers such as date palm (19.9%) [73] and *Arecanut hust* fibers (37.0%) [74]. A higher crystalline index indicates well-oriented cellulose crystals along the axis of the fiber.

In addition, the crystallite size (*D*) values found by Scherrer's equation were 3.54 nm and 1.8 nm of (LAF), and (SHAF) fibers, respectively. The crystallite size of LAF is 3.54 nm which is quite higher than the Shwetark fibers (3 nm), Nerium oleander (2.23 nm), flax (2.8 nm) and Hibiscus vitifolius (2.09 nm) [75, 76]. Also, the crystallite size (D) of SHAF, which is much greater than that determined for the Leucaena Leucocephala Tree fiber (1.6 nm) [77] and Kigelia africana fibers (1.73 nm) [78]. Less crystallite size attracts more water absorption characteristics of the fibers and is associated with amorphous constituents present in the fibers [75].

The spacing between the (200) planes (*d*) was calculated using the Bragg's Eq. (3). (*d*) is the spacing between the planes in the atomic lattice, and θ is the angle between the incident ray and the scattering planes [79]. The d-spacings of (LAF) and (SHAF) were 4.10 and 4.17A°, respectively. Similar results were observed by Oudiani et al. [80].

TGA and DTG analysis

Figure 4a and c shows the TGA and DTG analysis of the LAF and SHAF. A weight loss of LAF and SHAF of about 6 and 8%, respectively, was observed at the range of 30 to 122 °C. This could be explained by the evaporation of the water or the other volatile components present in the fibers [66, 81]. The first appears at the range of (229 to 272 °C) and (201–261 °C) are centered at 244.5 °C and 242.8°C of the LAF and SHAF with 3.9% and 21.0% of weight loss, respectively. These peaks can be predicated to the decomposition of hemicellulose, pectin and the glycoside linkages of [82]. The second peak observed at the range of 272 °C

Table 2 XDR parameters of LAF and SHAF

	2θ (200)	FWHM (°)	Crystallinity index (%)	Lattice spacing (*d*) (A°)	Crystal size (*D*) (nm)
LAF	21.59	2.23	51.0	4.10	3;57
SHAF	21.24	4.42	30.4	4.17	1.80

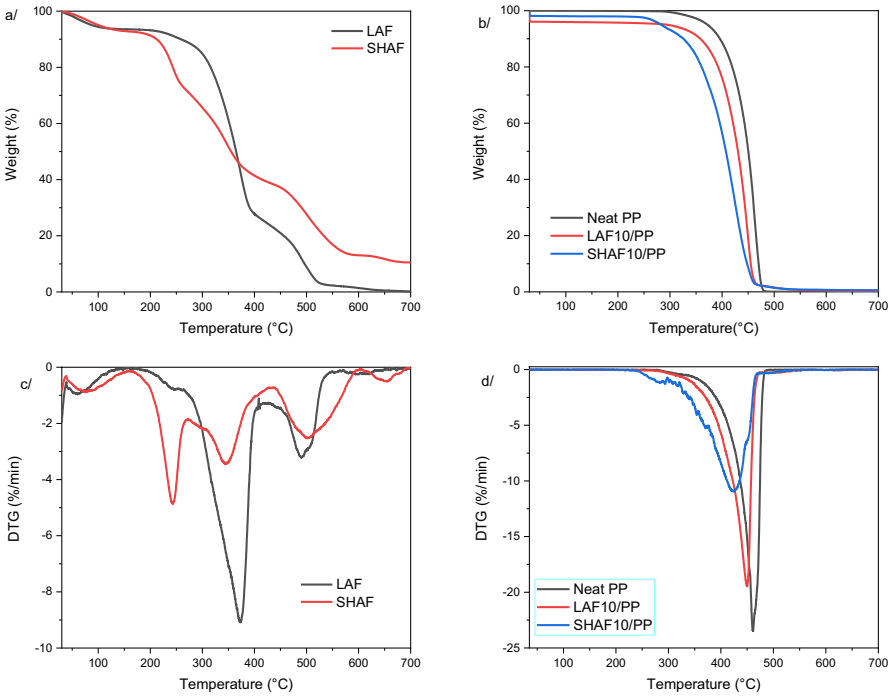

Fig. 4 TGA curve of **a** LAF and SHAF **b** Neat PP, LAF10/PP and SHAF10/PP and DTG curves of **c** LAF and SHAF **d** neat PP, LAF10/PP and SHAF10/PP

to 423 °C and 261 to 433 °C centered at 373 and 346 °C of LAF and SHAF can be due to the decomposition of cellulose [83]. Finally, the third small peak was observed at 488 °C and 500 °C of LAF and SHAF, respectively, and could be due to the decomposition of lignin [84]. The fourth peak at 653 °C of SHAF can be assigned to the decomposition of the molecules CO_2, CO, hydrocarbons and hydrogen [64].

As depicted in Fig. 4b and d, TGA and DTG curves show the thermal stability of neat PP, LAF10/PP and SHAF10/PP. The addition of LAF into PP matrix increased slightly the thermal stability as shown in Fig. 8, from 275.4 °C for the neat PP to 278.9 °C for LAF10/PP. This increase was correlated with the thermal protection that means the thermally more stable PP that surrounded the fiber. In addition, this enhancement in thermal stability was attributed to the better interaction between the PP and LAF. The addition of SHAF to the neat PP decreased the degradation temperature from 275.4 °C for the neat PP to 244.4 °C for the SHAF10/PP. The difference in thermal degradation between LAF and SHAF composites could probably due to the difference in chemical composition of these two fibers. LAF has lower content of lignin, while SHAF is rich in lignin [85]. Furthermore, the cellulose content in SHAF is much lower than that of LAF. Hence, the thermal stability of LAF was higher than that of SHAF. To conclude, the addition of the LAF in the PP improved the thermal stability of the composites.

Mechanical properties of composite

The tensile strength and the Young's modulus of the neat PP, LAF10/PP and SHAF10/PP (10 wt.%) composites are shown in Fig. 5. The composites containing SHAF and LAF showed better mechanical properties compared to the neat PP. The tensile strength increased up to 23.3 MPa and 19.6 MPa for LAF10/PP and SHAF10/PP, respectively, while it was 7.2 MPa for neat PP. The tensile modulus was 155 MPa for the neat PP and increased to 625 MPa with LAF and 440 MPa with SHAF. Composites reinforced with LAF exhibit higher tensile properties (Tensile strength and modulus) than composites reinforced with SHAF. This might be related to the increase in crystallinity of LAF already observed by the X-ray analysis compared to SHAF. Moreover, even the high cellulose contents of fibers have an important impact on composite properties, the improved performance can be related to the enhancement of fiber/matrix interaction. These observations confirm previous findings found by Haddar et al. [86]. Therefore, providing a better fiber/matrix interface, result to a more efficient stress transfer from the matrix to the fibers. However, compared to the neat PP, composites reinforced with LAF and SHAF exhibited lower elongation at break. It was 522.0% for neat PP and decreased to 23.0% and 14.5% of LAF10/PP and SHAF10/PP, respectively. This can be explained by stiffness effect of the fibers.

Nevertheless, from the results already published in the literature, the utilization of Agave (Agave tequilana) fibers as reinforcement for thermoplastic matrix led to remarkable decrease in elongation at break [50]. According to Boussetta et al., the use of rigid fibers to prepare composite materials in thermoplastic matrix leads to less deformability thanks to its low plastic energy that can be absorbed [87].

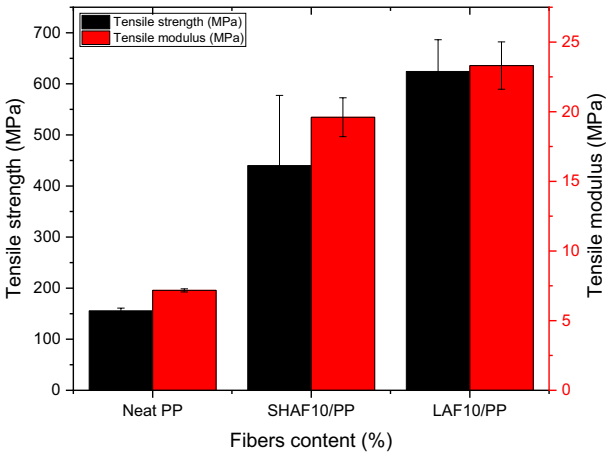

Fig. 5 Tensile strength and modulus of neat PP, LAF10/PP and SHAF10/PP

Water absorption

The water absorption behavior of the neat PP, LAF10/PP and SHAF10/PP composites with 10 wt% of agave fiber content was studied for 18 days, and results are depicted in Fig. 6. All samples showed the continuous rise in water uptake till 12 days. After 1 day less than 0.5% of water absorption was observed for neat PP, LAF10/PP and SHAF10/PP composites. Then, water absorption was suddenly increased and stabilized almost at the twelfth day. SHAF10/PP showed significantly higher water absorption than LAF10/PP. This increase in water absorption could be explained to the presence of higher amount of non-cellulosic materials (hemicelluloses and pectin) which had an hydrophilic character. In addition, the water absorption mechanism was related to the (–OH) groups that have the ability to bind with water, to the fiber structure that contains the capillary pores and even to the infiltration into the free space due to micro-voids and other morphological defects [88]. Saturated water weight for neat PP, LAF10/PP and SHAF10/PP was recorded as 0.6, 2.2 and 2.8%, respectively.

Density test

The low density is the major advantage that presents the cellulosic fibers over the synthetic ones (e.g., 2500 kg/m^3 for glass fiber) [89]. Cellulosic fibers contain pores and voids; hence, the low density is related to their porous nature. This advantage

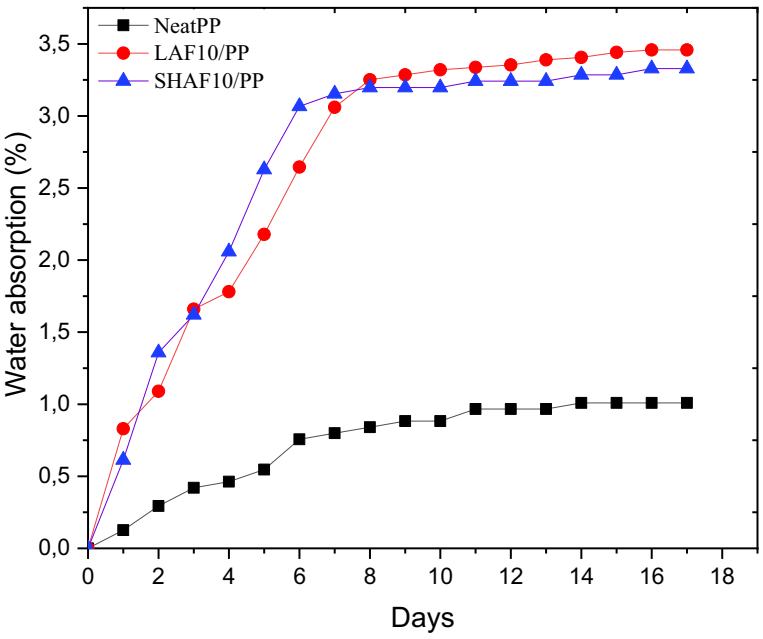

Fig. 6 Moisture absorption behavior of neat PP, LAF10/PP and SHAF10/PP

allows for using the natural fibers as reinforcement in polymer matrix, which may appreciably create low weight green composites. The LAF and SHAF density obtained from pycnometer are about 1.28 and 1.18 g/cm^3, respectively. The lower rate of hemicelluloses and lignin in the fibers increased the fiber density [90]. The chemical composition study confirms the decrease in non-cellulosic compounds of LAF compared to the SHAF which increased the density of LAF. In addition, the difference existing between the densities of cellulosic fibers is due to many parameters such as plant growth rate, climatic conditions (weather), plant tissue [63], extraction process, and porous rate of the microstructure [83].

The density (1.40 g/cm^3 of LAF10/PP and 1.33 g/cm^3 of SHAF10/PP) is higher than neat PP (0.94 g/cm^3). The good contact between both phases leads to a reduction in voids and defects, which could probably increase the density of the composites.

Differential scanning calorimetry (DSC)

The melting behavior of the composites was analyzed using differential scanning calorimetry (DSC) as illustrated in Fig. 7. The corresponding data comprising melting temperature T_f (°C), melting enthalpy (ΔH_f), and percentage of crystallinity (X_c%) of the composites. Table 2 shows that the crystallinity increased from 33.2% (PP) to 37.2% (LAF10/PP). The increase in crystallinity of LAF composite compared to SHAF composite implies that the first has more thermally stable crystals [91]. The slight decrease in crystallinity from 33.2% (neat PP) to 32.9% (SHAF10/PP) may be due to the presence of non-cellulosic compounds on the fiber surface, which can reduce nucleation effects of fibers. The crystallization temperature (T_c) of LAF10/PP and SHAF10/PP composites was lower than the neat PP. This could explained by the presence of fibers agglomeration during composite manufacturing,

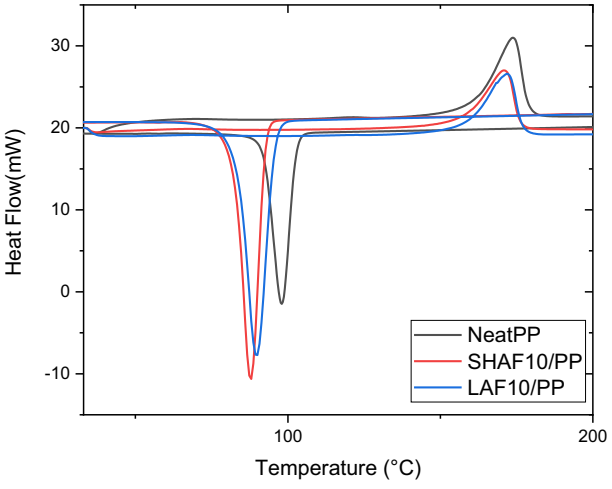

Fig. 7 DSC of neat PP, LAF10/PP and SHAF10/PP

where agglomerates lower the number of nucleating sites [92]. For the melting temperature (T_f), no significant changes were appeared.

Scanning electron microscopy (SEM)

The scanning electron microscopy provides a detailed idea about the morphology of LAF and SHAF surface to evaluate the fiber surfaces. The morphological analysis is important to predict fiber interaction with the polymer matrix in composites. As shown in Fig. 8a, the LAF contained a rough surface with the cracks. The occurrence of such cracks was attributed to the crystalline character of the fiber [93]. The crystalline character has a positive effect in the tensile properties of individual fiber, resulted in improving the mechanical properties of composites [94]. Consequently, the surface roughness will increase the fiber-matrix interfacial adhesion during the production of composites. The SHAF was mixed with powder and lignocellulosic fibers (Fig. 8b). The fibers showed in the SHAF surface contained rough surface and impurities in the form white layers and rectangular.

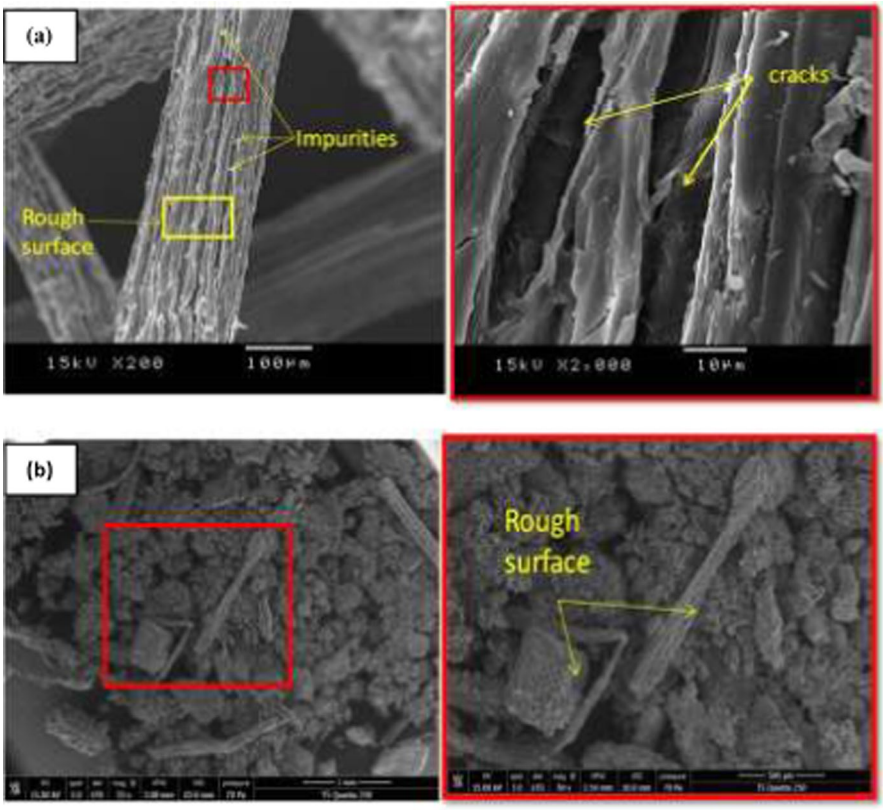

Fig. 8 SEM images of **a** LAF and **b** SHAF

Figure 9a–c shows SEM images of the fractured surfaces after the tensile test for the neat PP, SHAF10/PP and LAF10/PP, respectively, of the agave fibers composites. Figure 9a shows the rough surface. In Fig. 9b, the voids over the surfaces, pull-out and depending of some *Agave* fibers can be seen in the SHAF10/PP, which indicated the poor interfacial adhesion of SHAF10/PP. The void seen between the fibers and the matrix significantly affected the mechanical properties of SHAF10/PP. Figure 9c shows a better interfacial adhesion between LAF and PP. It is clear that the fibers are well incorporated in the matrix, and they exhibited a good dispersion at the microscopic scale. In fact, there was no indication that shows the fiber agglomeration on the studied fracture surfaces. In addition, it is also observed that the fibers were broken during fracture and reduced pull-out, which clearly indicates the good adhesion between the LAF and PP. This result is expected to produce a clear improvement in the mechanical properties of LAF10/PP due to good fiber dispersion that provides an efficient charge transfer from matrix to fibers [95, 96]. Not

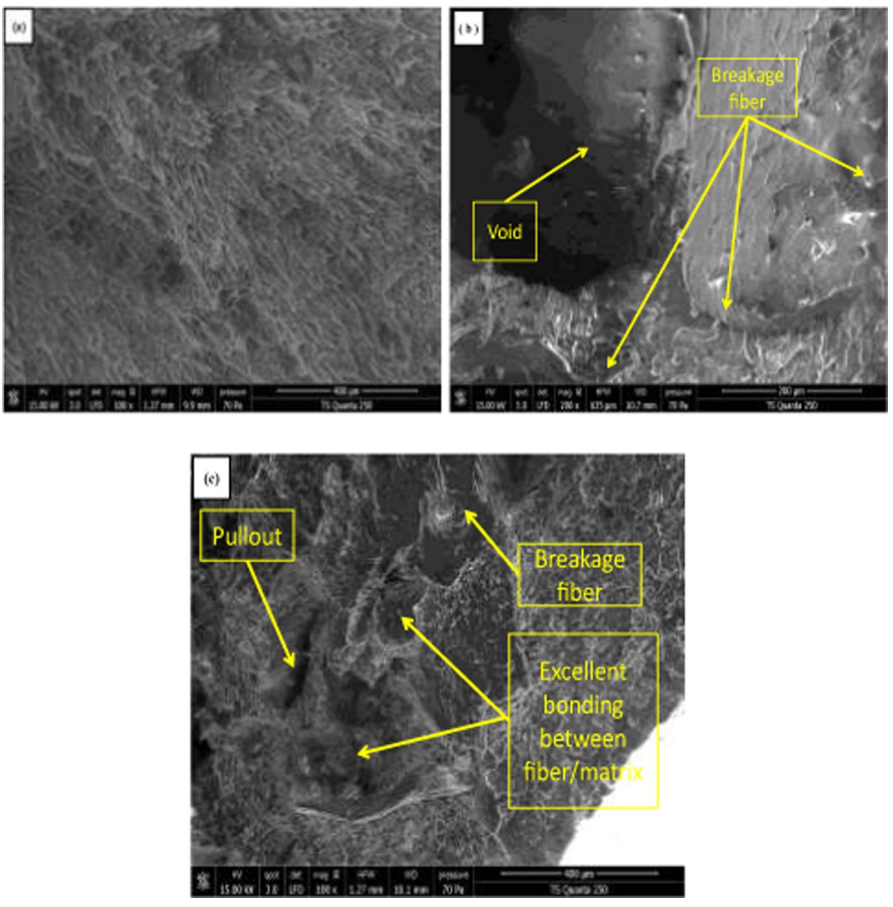

Fig. 9 SEM images of **a** neat PP **b** LAFPP/10 and **c** SHAF10/PP

only that, also the absence of agglomeration decreases stress concentrations in the composite, which leads to significant improvements in mechanical properties [97].

Conclusion

In the present investigation, composite based on PP matrix containing LAF and SHAF as fillers was successfully produced by twin-screw extruder and injection molding process. The filler content for both composites was chosen as 10 wt%. It was found that mechanical properties of the composites increased as compared to the neat PP. It was also noted that the tensile properties of LAF10/PP were higher than SHAF10/PP. This was due to the better thermal stability as well as to the higher cellulose content and crystallinity index of LAF that implies better interfacial adhesion between the fiber and the PP matrix. Hence, involving the chemical modification of SHAF or/and the use of coupling agent could be studied in subsequent research on the topic to improve the overall properties of this composite.

Declarations

Conflict of interest The authors declare no conflict of interest.

References

1. Estaji S, Paydayesh A, Mousavi SR et al (2021) Polycarbonate/poly(methyl methacrylate)/silica aerogel blend composites for advanced transparent thermal insulations: mechanical, thermal, and optical studies. Polym Compos 42:5323–5334. https://doi.org/10.1002/pc.26226
2. Mousavi SR, Faraj Nejad S, Jafari M, Paydayesh A (2021) Polypropylene/ethylene propylene diene monomer/cellulose nanocrystal ternary blend nanocomposites: effects of different parameters on mechanical, rheological, and thermal properties. Polym Compos 42:4187–4198. https://doi.org/10.1002/pc.26137
3. Razavi M, Sadeghi N, Jafari SH et al (2022) Thermo-rheological probe of microstructural evolution and degradation pathway in the flame-retarded PP/EVA/NOR/clay nanocomposites. Rheol Acta 61:25–47. https://doi.org/10.1007/s00397-021-01309-w
4. Mousavi SR, Estaji S, Raouf Javidi M et al (2021) Toughening of epoxy resin systems using core–shell rubber particles: a literature review. J Mater Sci 56:18345–18367. https://doi.org/10.1007/s10853-021-06329-8
5. Liu T, Huang K, Li L et al (2019) High performance high-density polyethylene/hydroxyapatite nanocomposites for load-bearing bone substitute: fabrication, in vitro and in vivo biocompatibility evaluation. Compos Sci Technol 175:100–110. https://doi.org/10.1016/j.compscitech.2019.03.012
6. Zhang C, Liu X, Liu H et al (2019) Multi-walled carbon nanotube in a miscible PEO/PMMA blend: thermal and rheological behavior. Polym Test 75:367–372. https://doi.org/10.1016/j.polymertesting.2019.03.003
7. Jiang L, He C, Fu J, Li X (2018) Wear behavior of alkali-treated sorghum straw fiber reinforced polyvinyl chloride composites in corrosive water conditions. Bio Resources 13(2):3362–3376
8. Singha AS, Rana RK (2013) Preparation and properties of agave fiber-reinforced polystyrene composites. J Thermoplast Compos Mater 26(4):513–526. https://doi.org/10.1177/0892705711425848
9. Shi X, Yang P, Peng X et al (2019) Bi-phase fire-resistant polyethylenimine/graphene oxide/melanin coatings using layer by layer assembly technique: smoke suppression and thermal stability of flexible polyurethane foams. Polymer 170:65–75. https://doi.org/10.1016/j.polymer.2019.03.008

10. Sullins T, Pillay S, Komus A, Ning H (2017) Hemp fi ber reinforced polypropylene composites: the effects of material treatments. Compos B 114:15–22. https://doi.org/10.1016/j.compositesb.2017.02.001
11. Raza ZA, Riaz S, Banat IM (2018) Polyhydroxyalkanoates: Properties and chemical modification approaches for their functionalization. Biotechnol Prog 34:29–41. https://doi.org/10.1002/btpr.2565
12. Riaz S, Rhee KY, Park SJ (2021) Polyhydroxyalkanoates (Phas): biopolymers for biofuel and biorefineries. Polymers 13:1–21. https://doi.org/10.3390/polym13020253
13. Qu M, Nilsson F, Qin Y et al (2017) Electrical conductivity and mechanical properties of melt-spun ternary composites comprising PMMA, carbon fibers and carbon black. Compos Sci Technol 150:24–31. https://doi.org/10.1016/j.compscitech.2017.07.004
14. Wang X, Pan Y, Qin Y et al (2018) Creep and recovery behavior of injection-molded isotactic polypropylene with controllable skin-core structure. Polym Test 69:478–484. https://doi.org/10.1016/j.polymertesting.2018.05.040
15. Pan Y, Guo X, Zheng G et al (2018) Shear-induced skin-core structure of molten isotactic polypropylene and the formation of β-crystal. Macromol Mater Eng 303(6):1800083. https://doi.org/10.1002/mame.201800083
16. Fu S, Yu B, Tang W et al (2018) Mechanical properties of polypropylene composites reinforced by hydrolyzed and microfibrillated Kevlar fibers. Compos Sci Technol 163:141–150. https://doi.org/10.1016/j.compscitech.2018.03.020
17. Zhang X, Wang X, Liu X et al (2018) Porous polyethylene bundles with enhanced hydrophobicity and pumping oil-recovery ability via skin-peeling. ACS Sustain Chem Eng 6(10):12580–12585. https://doi.org/10.1021/acssuschemeng.8b03305
18. Zhang F, Liu X, Zheng G et al (2018) Facile route to improve the crystalline memory effect: electrospun composite fiber and annealing. Macromol Chem Phys 219(17):1800236. https://doi.org/10.1002/macp.201800236
19. Panaitescu DM, Nicolae CA, Vuluga Z et al (2016) Influence of hemp fibers with modified surface on polypropylene composites. J Ind Eng Chem 37:137–146. https://doi.org/10.1016/j.jiec.2016.03.018
20. Jiang J, Liu X, Lian M et al (2018) Self-reinforcing and toughening isotactic polypropylene via melt sequential injection molding. Polym Test 67:183–189. https://doi.org/10.1016/j.polymertesting.2018.03.005
21. Liu X, Pan Y, Zheng G et al (2018) Overview of the experimental trends in water-assisted injection molding. Macromol Mater Eng 303(8):1800035. https://doi.org/10.1002/mame.201800035
22. Taktak I, Mansouri A, Souissi S, Etoh MA, Elloumi A (2023) Biocomposites films based on polylactic acid and olive wood-flour: investigation on physical, thermal and mechanical properties. J Elastom Plast. https://doi.org/10.1177/00952443231165426
23. Rosli NA, Ahmad I, Abdullah I et al (2015) Hydrophobic modification of cellulose isolated from *Agave angustifolia* fibre by graft copolymerisation using methyl methacrylate. Carbohyd Polym 125:69–75. https://doi.org/10.1016/j.carbpol.2015.03.002
24. Hamdi SE, Delisée C, Malvestio J et al (2015) X-ray computed microtomography and 2D image analysis for morphological characterization of short lignocellulosic fibers raw materials: a benchmark survey. Compos A Appl Sci Manuf 76:1–9. https://doi.org/10.1016/j.compositesa.2015.04.019
25. Taktak I, Mansouri A, Guerfali M et al (2023) Active bio composites films based on PLA/olive wood flour (*Olea europaea* L.)/cinnamon essential oil. Polym Bull. https://doi.org/10.1007/s00289-023-04737-1
26. Abraham E, Deepa B, Pothan LA et al (2011) Extraction of nanocellulose fibrils from lignocellulosic fibres: a novel approach. Carbohyd Polym 86:1468–1475. https://doi.org/10.1016/j.carbpol.2011.06.034
27. Sapuan SM, Pua FL, El-Shekeil YA, Al-Qqla FM (2013) Mechanical properties of soil buried kenaf fibre reinforced thermoplastic polyurethane composites. Mater Des 50:467–470. https://doi.org/10.1016/j.matdes.2013.03.013
28. Munawar SS, Umemura K, Kawai S (2007) Characterization of the morphological, physical, and mechanical properties of seven nonwood plant fiber bundles. J Wood Sci 53:108–113. https://doi.org/10.1007/s10086-006-0836-x
29. le Xu Y, Dayo AQ, Wang J et al (2018) Mechanical and thermal properties of a room temperature curing epoxy resin and related hemp fibers reinforced composites using a novel in-situ generated curing agent. Mater Chem Phys 203:293–301. https://doi.org/10.1016/j.matchemphys.2017.10.004

30. Akin DE, Condon B, Sohn M et al (2007) Optimization for enzyme-retting of flax with pectate lyase. Ind Crops Prod 25:136–146. https://doi.org/10.1016/j.indcrop.2006.08.003
31. Reddy N, Yang Y (2005) Biofibers from agricultural byproducts for industrial applications. Trends Biotechnol 23:22–27. https://doi.org/10.1016/j.tibtech.2004.11.002
32. Thamae T, Marien R, Chong L et al (2008) Developing and characterizing new materials based on waste plastic and agro-fibre. J Mater Sci 43:4057–4068. https://doi.org/10.1007/s10853-008-2495-3
33. Bilba K, Arsene MA, Ouensanga A (2007) Study of banana and coconut fibers. Botanical composition, thermal degradation and textural observations. Biores Technol 98:58–68. https://doi.org/10.1016/j.biortech.2005.11.030
34. Hulle A, Kadole P, Katkar P (2015) *Agave Americana* leaf fibers. Fibers 3(1):64–75
35. Msahli S, Ydrean J, Sakli F (2005) Evaluating the fineness of *Agave Americana* L. Fibers Text Res J 75(7):540–543. https://doi.org/10.1177/0040517505053808
36. Deghboudj S, Boukhedena W, Satha H (2023) Optimization of bending and compressive strength behavior of *Agave americana* fiber reinforced cementitious composite using response surface methodology. Period Polytech Civ Eng 67:744–756. https://doi.org/10.3311/ppci.21696
37. Mylsamy K, Rajendran I (2011) The mechanical properties, deformation and thermomechanical properties of alkali treated and untreated Agave continuous fibre reinforced epoxy composites. Mater Des 32:3076–3084. https://doi.org/10.1016/j.matdes.2010.12.051
38. Mansouri A, Ben Nasr J, Ben Amar M, Elhalouani F (2020) Characterization of fiber extracted from *Agave americana* after burial in soil. Fibers Polym 21:724–732. https://doi.org/10.1007/s12221-020-8666-9
39. Jaouadi M, Msahli S, Sakli F (2011) A study of the physical and mechanical properties of paper made from *Agave americana* L. fibers. Mater Manuf Process 26:567–572. https://doi.org/10.1080/10426910903124878
40. Bessadok A, Roudesli S, Marais S et al (2009) Etude et caracterisation des fibres d'alfa et d'agave modifiees chimiquement en vue de les incorporer dans un composite amatrice polyester. Compos A Appl Sci Manuf 40:184–195. https://doi.org/10.1016/j.compositesa.2008.10.018
41. Ortega Z, Castellano J, Suárez L et al (2019) Characterization of *Agave americana* L. plant as potential source of fibres for composites obtaining. SN Appl Sci 1:1–9. https://doi.org/10.1007/s42452-019-1022-2
42. Thamarai Selvi S, Sunitha R, Ammayappan L, Prakash C (2023) Impact of chemical treatment on surface modification of *Agave Americana* fibres for composite application—a futuristic approach. J Nat Fibers. https://doi.org/10.1080/15440478.2022.2142726
43. Bessghaier A, Oudiani EL (2010) Contribution à l ' étude du comportement mécanique des fibres d ' *Agave Americana* L.
44. Mylsamy K, Rajendran I (2011) Influence of alkali treatment and fibre length on mechanical properties of short Agave fibre reinforced epoxy composites. Mater Des 32:4629–4640. https://doi.org/10.1016/j.matdes.2011.04.029
45. Henriksson G, Akin DE, Hanlin RT et al (1997) Identification and retting efficiencies of fungi isolated from dew-retted flax in the United States and Europe. Appl Environ Microbiol 63:3950–3956
46. Akin DE (2013) Linen most useful: perspectives on structure, chemistry, and enzymes for retting flax. ISRN Biotechnol 2013:23. https://doi.org/10.5402/2013/186534
47. Pickering KL, Efendy MGA, Le TM (2016) A review of recent developments in natural fibre composites and their mechanical performance. Compos Part A 83:98–112. https://doi.org/10.1016/j.compositesa.2015.08.038
48. Torres-tello EV, Robledo-ortíz JR, González-garcía Y et al (2017) Effect of agave fiber content in the thermal and mechanical properties of green composites based on polyhydroxybutyrate or poly (hydroxybutyrate-co-hydroxyvalerate). Ind Crops Prod 99:117–125. https://doi.org/10.1016/j.indcrop.2017.01.035
49. Cisneros-l EO (2016) Rotomolded polyethylene-agave fiber composites: effect of fiber surface treatment on the mechanical properties. Polym Eng Sci 56(8):856–865. https://doi.org/10.1002/pen
50. Edén D, Denis RRG, Omar E et al (2017) Polylactic acid—agave fiber biocomposites produced by rotational molding: a comparative study with compression molding. Adv Polym Technol 37(7):2528–2540. https://doi.org/10.1002/adv.21928
51. Segal L, Creely JJ, Martin AE, Conrad CM (1959) An empirical method for estimating the degree of crystallinity of native cellulose using the X-ray diffractometer. Text Res J 29(10):786–794. https://doi.org/10.1177/004051755902901003

52. Moshiul Alam AKM, Beg MDH, Yunus RM et al (2018) Modification of structure and properties of well-dispersed dendrimer coated multi-walled carbon nanotube reinforced polyester nanocomposites. Polym Test 68:116–125. https://doi.org/10.1016/j.polymertesting.2018.04.005
53. Alam AKMM, Beg MDH, Yunus RM (2017) Microstructure and fractography of multiwalled carbon nanotube reinforced unsaturated polyester nanocomposites. Polym Compos 38:E462–E471. https://doi.org/10.1002/pc.23911
54. Mustafa WA, Saidi SA, Zainal M, Santiagoo R (2018) Experimental study of composites material based on thermal analysis. J Adv Res Fluid Mech Therm Sci 43:37–44
55. Morán-Velázquez DC, Monribot-Villanueva JL, Bourdon M et al (2020) Unravelling chemical composition of agave spines: news from *Agave fourcroydes* Lem. Plants 9:1–15. https://doi.org/10.3390/plants9121642
56. Madhu P, Sanjay MR, Jawaid M et al (2020) A new study on effect of various chemical treatments on *Agave Americana* fiber for composite reinforcement: physico-chemical, thermal, mechanical and morphological properties. Polym Testing 85:106437. https://doi.org/10.1016/j.polymertesting.2020.106437
57. Manimaran P, Senthamaraikannan P, Sanjay MR, Marichelvam MK (2018) Study on characterization of Furcraea foetida new natural fiber as composite reinforcement for lightweight applications. Carbohyd Polym 181:650–658. https://doi.org/10.1016/j.carbpol.2017.11.099
58. El Oudiani A, Chaabouni Y, Msahli S, Sakli F (2012) Mercerization of *Agave americana* L. fibers. J Text Inst 103(5):565–574. https://doi.org/10.1080/00405000.2011.590010
59. Saravanakumar SS, Kumaravel A, Nagarajan T et al (2013) Characterization of a novel natural cellulosic fiber from *Prosopis juliflora* bark. Carbohyd Polym 92(2):1928–1933. https://doi.org/10.1016/j.carbpol.2012.11.064
60. Kumar R, Hynes NRJ, Senthamaraikannan P et al (2018) Physicochemical and thermal properties of *Ceiba pentandra* bark fiber. J Nat Fibers 15:822–829. https://doi.org/10.1080/15440478.2017.1369208
61. Indran S, Raj RE (2015) Characterization of new natural cellulosic fiber from *Cissus quadrangularis* stem. Carbohyd Polym 117:392–399. https://doi.org/10.1016/j.carbpol.2014.09.072
62. Yang Q, Pan X (2012) Pretreatment of *Agave americana* stalk for enzymatic saccharification. Biores Technol 126:336–340. https://doi.org/10.1016/j.biortech.2012.10.018
63. Sathishkumar TP (2013) Characterization of new cellulose *Sansevieria ehrenbergii* fibers for polymer composites. Compos Interfaces 20(8):575–593. https://doi.org/10.1080/15685543.2013.816652
64. Indran S, Raj RE, Sreenivasan VS (2014) Characterization of new natural cellulosic fiber from *Cissus quadrangularis* root. Carbohyd Polym 110:423–429. https://doi.org/10.1016/j.carbpol.2014.04.051
65. De Rosa IM, Kenny JM, Puglia D et al (2010) Morphological, thermal and mechanical characterization of okra (*Abelmoschus esculentus*) fibres as potential reinforcement in polymer composites. Compos Sci Technol 70(1):116–122. https://doi.org/10.1016/j.compscitech.2009.09.013
66. Ganeshan P, NagarajaGanesh B, Ramshankar P, Raja K (2018) *Calotropis gigantea* fibers: a potential reinforcement for polymer matrices. Int J Polym Anal Charact 23(3):271–277. https://doi.org/10.1080/1023666X.2018.1439560
67. Porras A, Maranon A, Ashcroft IA (2015) Characterization of a novel natural cellulose fabric from *Manicaria saccifera* palm as possible reinforcement of composite materials. Compos B Eng 74:66–73. https://doi.org/10.1016/j.compositesb.2014.12.033
68. Reddy KO, Zhang J, Zhang J, Rajulu AV (2014) Preparation and properties of self-reinforced cellulose composite films from *Agave microfibrils* using an ionic liquid. Carbohyd Polym 114:537–545. https://doi.org/10.1016/j.carbpol.2014.08.054
69. De Rosa IM, Kenny JM, Maniruzzaman M et al (2011) Effect of chemical treatments on the mechanical and thermal behaviour of okra (*Abelmoschus esculentus*) fibres. Compos Sci Technol 71(2):246–254. https://doi.org/10.1016/j.compscitech.2010.11.023
70. French AD (2014) Idealized powder diffraction patterns for cellulose polymorphs. Cellulose 21:885–896. https://doi.org/10.1007/s10570-013-0030-4
71. Yanuhar U, Permanasari AA, Fikri AA et al (2017) Pulsed electric field assisted extraction of cellulose from mendong fiber (*Fimbristylis globulosa*) and its characterization. J Nat Fibers 15(3):406–415. https://doi.org/10.1080/15440478.2017.1330722
72. Subramanian K, Senthil Kumar P, Jeyapal P, Venkatesh N (2005) Characterization of ligno-cellulosic seed fibre from *Wrightia Tinctoria* plant for textile applications-an exploratory investigation. Eur Polym J 41:853–861. https://doi.org/10.1016/j.eurpolymj.2004.10.037

73. Pereira SC, Maehara L, Machado CMM, Farinas CS (2016) Physical-chemical-morphological characterization of the whole sugarcane lignocellulosic biomass used for 2G ethanol production by spectroscopy and microscopy techniques. Renew Energy 87:607–617. https://doi.org/10.1016/j.renene.2015.10.054
74. Jcc S, George N, Narayanankutty SK (2016) Isolation and characterization of cellulose nanofibrils from arecanut husk fibre. Carbohyd Polym 142:158–166. https://doi.org/10.1016/j.carbpol.2016.01.015
75. Raja K, Prabu B, Ganeshan P et al (2021) Characterization studies of natural cellulosic fibers extracted from shwetark stem. J Nat Fibers 18:1934–1945. https://doi.org/10.1080/15440478.2019.1710650
76. Manivel S, Pannirselvam N, Gopinath R, Sathishkumar TP (2022) Physico-mechanical, chemical composition and thermal properties of cellulose fiber from hibiscus vitifolius plant stalk for polymer composites. J Nat Fibers 19:6961–6976. https://doi.org/10.1080/15440478.2021.1941484
77. Gopinath R, Billigraham P, Sathishkumar TP (2023) Characterization studies on new cellulosic fiber extracted from *Leucaena Leucocephala* tree. J Nat Fibers. https://doi.org/10.1080/15440478.2022.2157922
78. Siva R, Valarmathi TN, Palanikumar K, Samrot AV (2020) Study on a novel natural cellulosic fiber from *Kigelia africana* fruit: characterization and analysis. Carbohyd Polym. https://doi.org/10.1016/j.carbpol.2020.116494
79. Yan Z, Chen S, Wang H et al (2008) Cellulose synthesized by *Acetobacter xylinum* in the presence of multi-walled carbon nanotubes. Carbohyd Res 343:73–80. https://doi.org/10.1016/j.carres.2007.10.024
80. El OA, Chaabouni Y, Msahli S, Sakli F (2011) Crystal transition from cellulose i to cellulose II in NaOH treated *Agave americana* L. fibre. Carbohyd Polym 86:1221–1229. https://doi.org/10.1016/j.carbpol.2011.06.037
81. Moshiul Alam AKM, Beg MDH, Reddy Prasad DM et al (2012) Structures and performances of simultaneous ultrasound and alkali treated oil palm empty fruit bunch fiber reinforced poly(lactic acid) composites. Compos A Appl Sci Manuf 43:1921–1929. https://doi.org/10.1016/j.compositesa.2012.06.012
82. Fiore V, Scalici T, Valenza A (2014) Characterization of a new natural fiber from *Arundo donax* L. as potential reinforcement of polymer composites. Carbohyd Polym 106:77–83. https://doi.org/10.1016/j.carbpol.2014.02.016
83. Belouadah Z, Ati A, Rokbi M (2015) Characterization of new natural cellulosic fiber from *Lygeum spartum* L. Carbohyd Polym 134:429–437. https://doi.org/10.1016/j.carbpol.2015.08.024
84. Nagarajaganesh B, Rengarajan M (2016) Physico-chemical, thermal, and flexural characterization of *Cocos nucifera* fibers. Int J Polym Anal Charact 21(3):244–250. https://doi.org/10.1080/1023666X.2016.1139359
85. Siakeng R, Jawaid M, Ariffin H, Sapuan SM (2018) Thermal properties of coir and pineapple leaf fibre reinforced polylactic acid hybrid composites. IOP Conf Ser Mater Sci Eng 368(1):012019. https://doi.org/10.1088/1757-899X/368/1/012019
86. Haddar M, Elloumi A, Koubaa A et al (2018) Synergetic effect of *Posidonia oceanica* fibres and deinking paper sludge on the thermo-mechanical properties of high density polyethylene composites industrial crops & products synergetic effect of *Posidonia oceanica* fibres and deinking paper sludge on. Ind Crops Prod 121:26–35. https://doi.org/10.1016/j.indcrop.2018.04.075
87. Boussetta A, Charii H, Ait Benhamou A et al (2023) Bio-composites based on cellulosic fibers from agro-industrial waste filled PP matrix: production and properties. Polym Bull. https://doi.org/10.1007/s00289-023-04698-5
88. Rahman WA, Nur S, Sudin A, Din SN (2012) Physical and mechanical properties of *Pandanus amaryllifolius* fiber reinforced low density polyethylene composite for packaging application. In: 2012 IEEE symposium on humanities, science and engineering research 345–349
89. Maheshwaran MV, Hyness NRJ, Senthamaraikannan P et al (2018) Characterization of natural cellulosic fiber from *Epipremnum aureum* stem. J Nat Fibers 15:789–798. https://doi.org/10.1080/15440478.2017.1364205
90. Sari NH, Wardana ING, Irawan YS et al (2017) Characterization of the chemical, physical, and mechanical properties of NaOH-treated natural cellulosic fibers from corn husks. J Nat Fibers 15(4):545–558. https://doi.org/10.1080/15440478.2017.1349707

91. Cisneros-López O, Anzaldo J, Fuentes-Talavera FJ et al (2015) Effect of agave fiber surface treatment on the properties of polyethylene composites produced by dry-blending and compression molding. Polym Compos 38(1):96–104
92. Perić M, Putz R, Paulik C (2019) Influence of nano fibrillated cellulose on the mechanical and thermal properties of poly (lactic acid). Eur Polym J 114:426–433. https://doi.org/10.1016/j.eurpolymj.2019.03.014
93. El Oudiani A, Chaabouni Y, Msahli S, Sakli F (2009) Physico-chemical characterisation and tensile mechanical properties of *Agave americana* L. fibres. J Text Inst 100(5):430–439. https://doi.org/10.1080/00405000701863350
94. Shanmugasundaram N, Rajendran I, Ramkumar T (2018) Characterization of untreated and alkali treated new cellulosic fiber from an Areca palm leaf stalk as potential reinforcement in polymer composites. Carbohyd Polym 195:566–575. https://doi.org/10.1016/j.carbpol.2018.04.127
95. Riaz S, Park SJ (2021) A comparative study on nanoinclusion effect of MoS2 nanosheets and MoS2 quantum dots on fracture toughness and interfacial properties of epoxy composites. Compos A Appl Sci Manuf 146:106419. https://doi.org/10.1016/j.compositesa.2021.106419
96. Riaz S, Park SJ (2020) Effective reinforcement of melamine-functionalized WS2 nanosheets in epoxy nanocomposites at low loading via enhanced interfacial interaction. Macromol Res 28:1116–1126. https://doi.org/10.1007/s13233-020-8151-8
97. Benhamou A, Boussetta A, Grimi N, El IM (2021) Characteristics of cellulose fibers from opuntia ficus indica cladodes and its use as reinforcement for PET-based composites characteristics of cellulose fibers from opuntia ficus indica cladodes and its use as reinforcement for PET based composites. J Nat Fibers 00:1–17. https://doi.org/10.1080/15440478.2021.1904484